Semi-Interpenetrated Polymer Networks Based On Modified Cellulose and Starch As Gel Polymer Electrolytes For High Performance Lithium Ion Batteries

Saeed Hadad
Sahand University of Technology
Mahtab Hamrahjoo
Sahand University of Technology
Elham Dehghani
Sahand University of Technology
Mehdi Salami-Kalajahi (m.salami@sut.ac.ir)
Sahand University of Technology https://orcid.org/0000-0002-8897-0997
Svetlana N. Eliseeva
Saint Petersburg State University Institute of Chemistry: Sankt-Peterburgskij gosudarstvennyj universitet Institut himii
Hossein Roghani-Mamaqani
Sahand University of Technology

Research Article

Keywords: Gel polymer electrolyte, Starch, Cellulose, Semi-interpenetrating polymer networks, Lithium ion battery

Posted Date: November 16th, 2021

DOI: https://doi.org/10.21203/rs.3.rs-1011029/v1

Version of Record: A version of this preprint was published at Cellulose on March 4th, 2022. See the published version at https://doi.org/10.1007/s10570-022-04468-y.

Abstract

Poly(ethylene oxide) (PEO) is one of the most famous polymer electrolytes; however, its low conductivity and capacity have prevented its commercial applications. This study utilizes carboxymethyl starch (CMS) and oxidative carboxymethyl cellulose (OCMC) natural polymers with a high potential to dissolve lithium ions (Li^+) in to help PEO ionic conductivity. The semi-interpenetrating polymer networks (semi-IPNs) consist of crosslinked poly(ethylene glycol) methyl ether methacrylate (PEGMA) with poly(ethylene glycol) diallyl (PEGDA) and free CMS/OCMC chains. Effect of increasing the amount of natural polymer on the electrochemical properties of semi-IPNs is investigated. Semi-IPN CMS50% and semi-IPN OCMC50% deliver excellent results such as high conductivity (in order 10^{-2} Scm^{-1}) at room temperature, electrochemical stability window higher than 4.5 V, high Li^+ transfer number, high discharge capacities (191 and 203 mAh g^{-1} with capacity retention of 85 and 88.5% after 100 cycles at 0.2 C, respectively), and stable cyclic behavior.

1. Introduction

Lithium ion batteries (LIBs) are widely utilized in electrical industry and energy storage devices because of their high energy density, lightweight, and stability (Hassoun et al. 2009; Zhou et al. 2014; Manthiram et al 2017). Typical LIBs use a highly conductive carbonate liquid as the electrolyte, whereas escape from these toxic and flammable solvents ends up in issues such as safety and contamination (Liu et al. 2018; Lisbona et al. 2011). Gel polymer electrolytes are one of the foremost effective ways that researchers have developed thus far for this downside besides increasing flexibility and mechanical properties of LIBs (Cho et al. 2019; Thakur et al. 2012; Lee et al. 2014). Poly(ethylene oxide) (PEO) is one of the most popular polymers used in GPEs (Zhang et al. 2019; Chan et al. 2018; Li et al. 2017), that has been studied a lot. However, because of its low ionic conductivity, deficient environmental friendly, and poor mechanical properties, it is not nevertheless become an acceptable alternative to liquid electrolytes (Zhou et al. 2019; Naderi et al. 2016). The solutions planned by the researchers are to use natural polymers with high electron donor atoms in their structure (Baskoro et al. 2019), equivalent to cellulose and its derivatives, and to blend them with synthetic polymers such as PEO, or to composite them with different polymers and fillers. Cellulose/PEG based GPE (Zhao et al. 2020), and GPE based on cellulose triacetate and poly(polyethylene glycol methacrylate) p(PEGMA) employing a photopolymerization technique(Nirmale et al. 2017), are instances of the blending approach. A cross-linked nanocomposite polymer electrolyte (CNPE) based on poly(propylene oxide)-poly(ethylene oxide)- poly(propylene oxide) triblock chains and surface-modified SiO_2 nanoparticles (Tang et al. 2020), nanocellulose/hydroxypropyl methylcellulose composite matrix as biodegradable, flameproof, and self-standing GPE (Gou et al. 2021), sandwich composite of PEO@$(Er_{0.5}Nb_{0.5})_{0.05}Ti_{0.95}O_2$@cellulose electrolyte (Zheng et al. 2021), cross-linked nano-SiO_2 and cellulose acetate (Hu et al. 2020), and GPE based on pure natural polymer matrix of potato starch composite lignocellulose (Song et al. 2017) are examples of composites. In a motivating study, Zhu *et al*. (Zhu et al. 2015) synthesized a porous membrane of carboxymethyl cellulose (CMC) by a simple nonsolvent evaporation method as a host of a GPE for LIBs. Despite these studies, the absence of

an effective and environmental friendly GPE for LIBs continues to be felt. Carboxymethyl starch (CMS) and oxidative carboxymethyl cellulose (OCMC) are two offered and environmental friendly natural polymers with high mechanical strength (due to high glass transition temperature (T_g)) (Heinze et al. 2005; Jiang et al. 2016; Cheng et al 2008). These two polymers have high potential for GPEs applications because of the large number of electron donor atoms in their repeating units. However, their smooth and nonporous surface prevents the whole uptake of lithium salt solution (Zhu et al. 2015; Minaev et al. 2016). As a result, these two polymers cannot show their potential in dissolving and transporting lithium salts as GPEs. To overcome this challenge, blending CMS/OCMC with other polymeric phases with high ability to uptake lithium salt solution such as cross-linked PEO is an effective approach (Dragan et al. 2014).

To require advantage of the utmost swelling properties of PEO and ionic conductivity of CMC/OCMC, this study synthesizes a GPE based on semi-interpenetrating polymer network (semi-IPN) structure. This consists of a crosslinked network of poly(ethylene glycol) methyl ether methacrylate (PEGMA)/poly(ethylene glycol) diallyl (PEGDA) (as a protracted chain crosslinker), and CMS/OCMC free chains. Herein, P(PEGMA) network helps uptaking lithium salt solution and CMS/OCMC additionally improves ion transfer beside mechanical properties of the ultimate GPE. Furthermore, effect of amount of natural polymers (CMS/OCMC) in the P(PEGMA)-PEGDA networks on the electrochemical properties similar to solvent uptake and conductivity is investigated. Finally, electrochemical properties and performance of fabricated lithium ion batteries are investigated.

2. Experimental Section

2.1. Synthesis of carboxymethyl cellulose (CMC) and oxidative carboxymethyl cellulose (OCMC)

Firstly, cellulose was extracted from cotton gin waste in 4 steps: treatment of cotton gin waste with NaOH (20 *wt%*), bleaching with H_2O_2 (1.5 *wt%*), adjusting the pH at 7 by dilute HCl, and acid treatment with H_2SO_4 (10 *wt%*). Then, cellulose was converted to CMC after alkalization and etherification with monochloroacetic acid and NaOH (Haleem et al. 2014). Subsequently, periodic acid was added to a clear solution of CMC and distilled water under stirring. Finally, the pH of the solution was adjusted to about 3.5 by using dilute H_2SO_4 and sodium bicarbonate at 45°C to obtain OCMC (Anjali et al. 2012).

2.2. Synthesis of carboxymethyl starch (CMS)

Starch and sodium monochloroacetate (1:1 w/w) were dissolved in NaOH solution (15%). Then, isopropyl alcohol was added to the solution under stirring and nitrogen purging at 40 ℃. After filtration, it was suspended in methanol and neutralized with acetic acid. At the end, the obtained slurry was dried in a vacuumed oven at 40 ℃ for 48 h (Lawal et al. 2007).

2.3. Synthesis of poly(ethylene glycol) diallyl (PEGDA)

PEG 600 (2 g, 1 mmol) was dissolved in THF (70 mL). Then, allyl bromide (173 µL, 2 mmol) was added dropwise to the reaction mixture at room temperature. Afterward, powder NaOH (200 mg, 5 mmol) was added to the mixture, and the resulting suspension was stirred at 80°C for 24 h. After cooling at room temperature, it was filtered and washed several times with THF to eliminate the catalyst. Subsequently, the aqueous solution was dried under vacuumed oven at room temperature (Mauri et al. 2015). Scheme S1 shows the synthetic approach of PEGDA.

2.4. Preparation of semi-IPN-PEGMA/OCMC and semi-IPN-PEGMA/CMS

PEGMA and OCMC in different molar ratios of 90/10, 70/30, and 50/50 were dissolved in distilled water. Then, synthesised PEGDA (10 *mol*. % of total monomer) was added to the reaction mixture. Subsequently, in situ polymerization was initiated by introduction of KPS (1 *mol*. % of total monomer) and mixtures were casted in Teflon molds. The reaction was continued for 5 h in an oven at 65 ℃. The obtained films were dried in a vacuumed oven at 35 ℃ overnight. The preparation of SIPN-PEGMA/CMS procedure was performed as SIPN-PEGMA/OCMC.

2.5. Preparation of GPE

The obtained films were swollen in 1 M solution of $LiPF_6$ in diethyl carbonate (DEC)/dimethyl carbonate (DMC) (1:1 V/V) for 1 h in a glove box and then utilized for further characterizations. Table 1 shows the coding of different GPEs.

Table 1
Composition of semi-IPNs Mixture

The ratio of semi-IPN-PEGMA/Polymer(w/w)	CMS	OCMC
100/0	PEGMA	PEGMA
90/10	semi-IPN CMS10%	semi-IPN OCMC10%
70/30	semi-IPN CMS30%	semi-IPN OCMC30%
50/50	semi-IPN CMS50%	semi-IPN OCMC50%

2.6. Electrochemical characterizations

Electrochemical impedance spectroscopy (EIS) was carried out using a PGE-18 electrochemical workstation to measure ionic conductivity of GPEs within a frequency range from 1 MHz to 0.1 Hz at an AC potential amplitude of 10 mV. The ionic conductivity of electrolytes was calculated according to Equation (1):

$$\sigma = \frac{h}{R_p A} \quad (1)$$

where σ is the ionic conductivity, R_p is the bulk resistance of polymer which is obtained by fitting the appropriate circuit on the Nyquist curves by ZsimpWin software, A is the area of the electrode–electrolyte interface, and h is the thickness of the polymer film. Also, temperature dependent conductivity was carried out at different temperatures. GPEs were sandwiched between two electrodes made up of stainless-steel (SS) for measurement of impedance. The cyclic voltammetry (CV) and the charge–discharge tests were performed by means of an Atomlab electrochemical workstation. CV curves were operated from 0.0 to 6.0 V for the $LiCoO_2$/GPE/Li cell at a scan rate of 0.1 mV s^{-1}. The galvanostatic charge and discharge (constant current) cycling tests were performed at ambient temperature in the potential window of 2.50 to 4.50 V at different rates on a Li/GPE/$LiCoO_2$. The cathode was used for CV and charge-discharge tests, comprised 80 *wt.* % $LiCoO_2$, 5 *wt.* % PVDF, and 15 *wt.* % super-P carbon black. All these materials were dissolved in NMP as solvent, then, the obtained slurry was coated on aluminum foil and vacuum-dried at 80°C for 24 h. Cell fabrication was accomplished in a glovebox filled with argon gas. To prepare cells, GPEs (A= 25 mm^2, h= 1.5 mm) were sandwiched between the above prepared $LiCoO_2$ cathode and lithium foil without any adhesion. DC polarization and impedance analysis were utilized to measure the transference number (t^+) of GPEs at 10 mV DC voltage which was applied to Li/GPE/Li cell. t^+ of electrolytes was calculated according to the Equation (2):

$$t_{Li+} = \frac{I_{ss}(\Delta V - I_0 R_{b.0})}{I_0(\Delta V - I_{ss} R_{b.ss})} \quad (2)$$

where I_0 is initial current, I_{ss} is steady state currents, $R_{b.0}$ is initial resistance, and $R_{b.ss}$ is final resistance which were measured by AC impedance spectroscopy. Electrochemical measurements, except for the temperature dependent conductivity were carried out at room temperature.

3. Results And Discussion

The synthesis of GPEs have been carried out according to the procedure mentioned in the Experimental Section and graphical illustration shown in Scheme 1.

To ensure correct synthesis of semi-IPNs, Fig. S1 shows the FT-IR spectra for PEGDA, PEGMA cross-linked networks (PEGMA-PEGDA), CMS, OCMC, semi-IPN CMS 50%, and semi-IPN OCMC 50%. PEGDA and PEGMA have similar FT-IR spectra because of their similar structures. In the spectra of PEGMA-PEGDA and PEGDA, the absorption peak at 1030 cm^{-1} is related to C-O stretching, 2869 cm^{-1} corresponded to CH vibration, and absorption peak at 3541 cm^{-1} is associated with absorbed humidity. In PEGMA-PEGDA spectra, peak at 1746 cm^{-1} belongs to the carbonyl end group of PEGMA monomers, and loss of PEGDA absorption peak at 951 and 1661 cm^{-1} in PEGMA-PEDGA related to =C-H out of plane bending and C=C starch, respectively, is a sign of the formation of PEGMA-PEGDA network. CMS and OCMC joint absorption peaks occur in 1102 cm^{-1} and 1030 cm^{-1} (C-O stretching), 1464 cm^{-1} (CH_2 scissoring), 2869 cm^{-1} (CH vibration), 3500 cm^{-1} (hydroxyl group), and 1750 cm^{-1} due to carbonyl group. The spectra of semi-IPNs are a combination of PEGMA-PEGDA and SMC/OCM spectra and no new peaks are added or

subtracted from, and this means the physical blending of PEGMA-PEGDA and CMS/OCMC together with no chemical bonding (Anjali et al. 2012; Lawal et al. 2007; Mauri et al. 2015; Lin et al. 2006; Brown et al. 2007; Pereira et al. 2011). To further prove the successful syntheses, ^{1}H NMR spectra of synthesized polymers are illustrated in Fig. S2 and peaks are assigned in detail.

DSC and XRD are utilized to confirm that the synthesized semi-IPNs are amorphous (Fig. 1). According to results, there is no peak related to ordered and crystalline structure in diffraction patterns of PEGMA, natural polymers, and semi-IPNs (Fig. 1a). Additionally, from the DSC curves, synthesized polymers and semi-IPNS are utterly amorphous and there is no indication of melting phenomenon (Fig. 1b). Moreover, T_g of semi-IPNs is increased with increasing CMS/OCMS content whereas it was between T_g of PEGMA and CMS/OCMC. This increase in T_g shows a positive deviation from Fox equation thanks to the strong interaction between these two phases (PEGMA-PEGDA network and CMS/OCMC) within the semi-IPNs. More deviation of semi-IPNs OCMC is due to the presence of carbonyl groups in the cellulose chain backbone and the possibility of creating more hydrogen interactions with P(PEGMA)-PEGDA network. This strong interaction between PEGMA and CMS/OCMC makes two components very compatible (Murthy et al. 1990; Prinos et al. 1995).

TGA is utilized to evaluate the thermal stability of the synthesized semi-IPNs (Fig. 2). TGA curves show approximately same thermal stability for PEGMA and OCMC up to 200°C, and high CMS thermal stability up to 345°C. Therefore, by increasing the amount of CMS in PEGMA network, the thermal stability of the semi-IPNs is improved. However, by increment of OCMC in PEGMA-PEGDA, thermal stability is not changed remarkable. Also, in each case, residual char is increased with an increasing quantity of natural polymers (CMS/OCMC) inside the polymer network (Jagadish et al. 2011; Rajeh et al. 2019).

As known, the ionic conductivity of a polymer electrolyte depends on two important factors: a) the quantity of polymeric host electron donor atoms, and b) the T_g, which controls the mobility of the polymer chains. More electron donor atoms contribute to the dissociation of lithium salts and lower T_g facilitates transfer of within the polymer host (Zhou et al. 2019). PEO incorporates a low T_g; however, it has one electron donor atom in each repeating unit whereas CMS and OCMC have at least 14 electron donor atoms in their structures. However, because of high T_g and a small amount of solvent uptake, they may not be effective in the GPEs. Here, the semi-IPN structure is employed to maximum utilization of the high mobility of PEO chains and also the high ability of CMS and OCMC to establish coordination with Li^{+}. To verify this supposition, electrochemical tests are performed and the impact of adding natural polymers (CMS or OCMC) to PEGMA network on the electrochemical behavior of the resulting electrolytes are investigated. Nyquist curves for semi-IPN CMS and semi-IPN OCMC with different amounts of CMS and OCMC and their ionic conductivity at different temperatures (from 25 to 65°C) are shown in Fig. 3. The results indicate a pointy decrease within the resistance of electrolytes by increasing the proportion of natural polymer. Semi-IPN CMS 50% and semi-IPN OCMC 50% show an ionic conductivity of $1.74*10^{-2}$ and $1.92*10^{-2}$ S cm^{-1}, respectively. The most GPEs show conductivity in the order of 10^{-3} S cm^{-1} and this is their main disadvantage compared to liquid electrolytes (Liu et al. 2020; Liu et al. 2021; Shen et al.

2020; Xue et al. 2021; Gou et al. 2020). However, here semi-IPN CMS and semi-IPN OCMC samples take the ionic conductivity of the GPEs one step further and makes them competitive with liquid electrolytes. The explanation for this high ionic conductivity is the presence of a large number of oxygen atoms within the CSM or OCMC in the electrolyte, that gives several sites prone to coordination with Li^+. So PEGMA chains permit lithium ions to move simply between these places due to their high mobility. As the amount of natural polymer in the network is increased, the ionic conductivity becomes greater while T_g is increased. This means that the number of electron donor atoms is more controlling than T_g of polymeric host in ionic conductivity. Due to the increase in T_g and more importantly, reduced salt solution uptake of the semi-IPNs, it is expected that higher amount of natural polymer leads to difficulty in transfer of ions, Semi-IPN 50% of CMS and OCMC show the most increase of ionic conductivity. In this regard, PEGDA, as a long-chain crosslinker, plays a crucial role in these results, and provides a regular, free-volume network that is appropriate for placing CMS/OCMC chains next to PEGMA and great salt solution uptake (Fig. S3). Higher ionic conductivity of OCMC-based semi-IPNs than CMS-based ones despite its higher T_g originates from greater importance of polar functional groups (carbonyl groups on OCMC backbone) on the ionic conductivity of the polymeric host.

The Arrhenius ionic conductivity behavior with temperature and low activation energy (E_a) of semi-IPNs is well clear (Baskoro et al. 2019). Moreover, the decrease of the temperature affect conductivity by increasing the CMS/OCMC content due to rise in T_g of semi-IPNs. The electrochemical stability window of GPEs based on semi-IPNs is critical for the practical application in LIBs. From cyclic voltammetry (CV) of semi-IPNs (Fig. 4a.), it is realized that there is no obvious oxidation current before 4.5 V for each semi-IPN CMS and semi-IPN OCMC, which is favorable for the feasible applications of semi-IPNs for high-potential electrolyte in LIBs (Shen et al. 2020). The stability window of both semi-IPNs is very close due to the similar structures. Li^+ transference number (t^+) as a vital parameter for evaluating the GPEs is the proportion of Li^+ transport to the total ions that transport within the polymer electrolyte. The low t^+ causes the maldistribution of ion concentration, polarization, and side reactions in GPEs (Lin et al. 2020). From the chronoamperometry and EIS tests in Fig. 4b, t^+ of semi-IPN CMS 50% and semi-IPN OCMC 50% is 0.655 and 0.8, respectively, which is far above the liquid and ordinary polymer electrolytes. The very high value of t^+ for semi-IPNs is due to the high ionic conductivity and Li electrode/electrolyte compatibility, which causes uniform solid electrolyte interface (SEI) (An et al. 2016). The oxygen atoms in the structure of OCMC/CMS create more coordination sites for Li^+, also are adapted to the volume expansion of lithium; and finally, the PEGMA chains accelerate the movement of Li^+ ions in these pathways.

Fig. 5 shows the initial charge-discharge curves of $LiCoO_2$/semi-IPN CMS50%/Li and $LiCoO_2$/semi-IPN OCMS50%/Li batteries assembled at different the current density (0.2, 0.5, 1, and 2 C). It can be seen that the initial discharge capacity of semi-IPN CMS50% and semi-IPN OCMS50% LIBs are 203 and 191.56 mAh g^{-1} at 0.2 C, respectively, which is far larger than the discharge capacity of polymer electrolyte-based LIBs even at 0.1 C current density (Lizundia et al. 2021; Dong et al. 2019; Ahmed et al. 2020; Yue et al. 2016). Increasing the current density limits the Li^+ kinetics and polarizes the battery, which results in

reducing the battery capacity. This is why most batteries perform well at low currents, whereas it increases the power and charge rate of the battery (Vetter et al. 2005). The synthesized GPEs here show a high specific capacity even at high current densities, thanks to their unique structures. The most PEO-based GPEs do not show stable cyclic performance due to the incompatibility of the electrode/electrolyte interface, and as a result of the expansion of dendrites at the anode surface, the battery discharge capacity gradually decreases throughout the charge-discharge cycle (Zhao et al. 2020). Fig. 5c displays the rate performances of LIBs versus current density from 0.2 to 2 C. The carbonyl and hydroxyl groups in CMS and OCMC increase the compatibility between the anode/electrolyte interfaces (Li et al. 2020), leading to a very stable charge-discharge cycle performance of the LIBs. The performance of charge-discharge cycles with 100 times at 0.2 C and coulombic efficiency (CE) of LIBs with semi-IPN CMS50% and semi-IPN OCMS50% are displayed in Fig. 7d. $LiCoO_2$/semi-IPN CMS50%/Li shows a CE ~ 88% at primary cycle with capacity retention of 85% after 100 cycles, and LIB based on semi-IPN-OCMC indicates CE ~ 92% and 88.5% capacity retention after 100 cycle. The interesting point is that the CE quickly reaches 100% and also the process of reducing the battery capacity is stopped in the same initial cycles. The prevalence of polymeric electrolyte over liquid one in addition to safety is the ability of the polymer to prevent dendritic growth because of its mechanical strength (Liu et al. 2018; Wang et al. 2019). Adding CMS/OCMC to the PEGMA cross-linked network in addition to increase the strength of the ultimate semi-IPN structure (by increasing electrolyte T_g), can also form suitable interface (polar functional groups in CMS and OCMC, can introduce lithium ion uniform deposition); as a result the resistance of the GPEs against dendritic expansion is increased.

To further investigation the effect of natural polymers on the dendrites growth, electrolyte (anode-side) surface is studied by FE-SEM images (Fig. 6). The surface pictures of the gels before the charge-discharge test show the right dispersion of the two phases inside each other, and after 100 charge-discharge cycles, the dendrites are seen scattered without accumulation (due to sensible interaction at the electrolyte/electrode interface) and tiny in size (indicates that the electrolyte prevents the expansion of dendrites) on the electrolyte surface.

4. Conclusion

In a nutshell, unique semi-IPNs combination of CMS/OCMC and PEGMA-PEGDA was used to prepare gel polymer electrolytes for high performance LIBs. Ionic conductivity was increased sharply due to the addition of a large number of electron donor atoms (CMS/OCMC chains) to the PEGMA-PEGDA network, reaching 1.74 and 1.92 S cm^{-1} for semi-IPN-CMS50% and semi-IPN-OCMC50%, respectively. With the addition of modified natural polymers to the PEGMA-PEGDA network, the strength of the electrolyte and its compatibility with the electrolyte was increased with subsequent stopping the dendrites expansion. These properties together, provided stable charge-discharge behavior, high t^+, and a supreme discharge capacity (195 and 184 mAh g^{-1} for SIPN-CMS50% and SIPN-OCMC50%, respectively) for both Semi-IPNs after 100 cycles. The approach presented here for polymeric electrolyte synthesis has the potential to produce sustainable, economical, and safe LIBs.

Declarations

Acknowledgements: This work is based upon research funded by Iran National Science Foundation (INSF) under project No. 99003725 and Russian Foundation for Basic Research (RFBR) under project No. 20-53-56069.

Data availability: The raw/processed data required to reproduce these findings cannot be shared at this time as the data also form part of an ongoing study.

Supporting information: Materials; Instrumental Analysis; ^{1}H NMR spectra; EIS results

CRediT author statement

Saeed Hadad: Methodology, Validation, Formal Analysis, Investigation, Writing – Original Draft, Visualization. **Mahtab Hamrahjoo**: Validation, Resources, Investigation, Writing – Original Draft, Visualization. **Elham Dehghani:** Methodology, Validation, Formal Analysis. **Mehdi Salami-Kalajahi:** Validation, Resources, Visualization, Writing – Review & Editing, Supervision, Funding Acquisition. **Svetlana N. Eliseeva:** Validation, Resources, Visualization, Writing – Review & Editing, Supervision, Funding Acquisition. **Hossein Roghani-Mamaqani**: Writing – Review & Editing, Visualization.

Conflict of Interest: The authors declare that they have no conflict of interest.

References

1. Anjali T (2012) Modification of carboxymethyl cellulose through oxidation. Carbohydr Polym 87(1):457–460. https://doi.org/10.1016/j.carbpol.2011.08.005
2. An SJ, Li J, Daniel C, Mohanty D, Nagpure S, Wood III, DL (2016) The state of understanding of the lithium-ion-battery graphite solid electrolyte interphase (SEI) and its relationship to formation cycling. Carbon 105:52–76. https://doi.org/10.1016/j.carbon.2016.04.008
3. Ahmed F, Choi I, Ryu T, Yoon S, Rahman MM, Zhang W, Jang H, Kim W (2020) Highly conductive divalent fluorosulfonyl imide based electrolytes improving Li-ion battery performance: Additive potentiating electrolytes action. J Power Sourc 455:227980. https://doi.org/10.1016/j.jpowsour.2020.227980
4. Baskoro F, Wong HQ, Yen HJ (2019) Strategic structural design of a gel polymer electrolyte toward a high efficiency lithium-ion battery. ACS Appl Energy Mater 2(6):3937–3971. https://doi.org/10.1021/acsaem.9b00295
5. Brown EE, Laborie MPG (2007) Bioengineering bacterial cellulose/poly (ethylene oxide) nanocomposites. Biomacromolecules 8(10):3074–3081. https://doi.org/10.1021/bm700448x
6. Cho YG, Hwang C, Cheong DS, Kim YS, Song HK (2019) Gel/solid polymer electrolytes characterized by in situ gelation or polymerization for electrochemical energy systems. Adv Mater 31(20):1804909. https://doi.org/10.1002/adma.201804909

7. Chen L, Li Y, Li SP, Fan LZ, Nan CW, Goodenough JB (2018) PEO/garnet composite electrolytes for solid-state lithium batteries: From “ceramic-in-polymer” to “polymer-in-ceramic”. Nano Energy 46:176–184. https://doi.org/10.1016/j.nanoen.2017.12.037
8. Cheng YQ, Sheng HW, Ma E (2008) Relationship between structure, dynamics, and mechanical properties in metallic glass-forming alloys. Phys Rev B 78(1):014207. https://doi.org/10.1103/PhysRevB.78.014207
9. Dragan ES (2014) Design and applications of interpenetrating polymer network hydrogels. A review. Chem Eng J 243:572–590. https://doi.org/10.1016/j.cej.2014.01.065
10. Dong D, Zhang H, Zhou B, Sun Y, Zhang H, Cao M, Li J, Chen H (2019) Porous covalent organic frameworks for high transference number polymer-based electrolytes. Chem Commun 55(10):1458–1461. https://doi.org/10.1039/C8CC08725C
11. Gou J, Liu W, Tang A, Xie H (2021) A phosphorylated nanocellulose/hydroxypropyl methylcellulose composite matrix: a biodegradable, flame-retardant and self-standing gel polymer electrolyte towards eco-friendly and high safety lithium ion batteries. Eur Polym J 110703. https://doi.org/10.1016/j.eurpolymj.2021.110703
12. Gou J, Liu W, Tang A (2020) A renewable gel polymer electrolyte based on the different sized carboxylated cellulose with satisfactory comprehensive performance for rechargeable lithium ion battery. Polymer 208:122943. https://doi.org/10.1016/j.polymer.2020.122943
13. Hassoun J, Panero S, Reale P, Scrosati B (2009) A new, safe, high-rate and high-energy polymer lithium-ion battery. Adv Mater 21(47):4807–4810. https://doi.org/10.1002/adma.200900470
14. Hu J, Liu Y, Zhang M, He J, Ni P (2020) A separator based on cross-linked nano-SiO2 and cellulose acetate for lithium-ion batteries. Electrochim Acta 334:135585. https://doi.org/10.1016/j.electacta.2019.135585
15. Heinze T, Koschella A (2005) March) Carboxymethyl ethers of cellulose and starch–a review. Macromolecular Symposia, vol 223. WILEY-VCH Verlag, Weinheim, pp 13–40. 1 https://doi.org/10.1002/masy.200550502.
16. Haleem N, Arshad M, Shahid M, Tahir MA (2014) Synthesis of carboxymethyl cellulose from waste of cotton ginning industry. Carbohydr Polym 113:249–255. https://doi.org/10.1016/j.carbpol.2014.07.023
17. Mauri E, Rossi F, Sacchetti A (2015) Simple and efficient strategy to synthesize PEG-aldehyde derivatives for hydrazone orthogonal chemistry. Polym Adv Technol 26(12):1456–1460. https://doi.org/10.1002/pat.3578
18. Jiang X, Yang Z, Peng Y, Han B, Li Z, Li X, Liu W (2016) Preparation, characterization and feasibility study of dialdehyde carboxymethyl cellulose as a novel crosslinking reagent. Carbohydr Polym 137:632–641. https://doi.org/10.1016/j.carbpol.2015.10.078
19. Jagadish RS, Raj B (2011) Properties and sorption studies of polyethylene oxide–starch blended films. Food Hydrocolloids 25(6):1572–1580. https://doi.org/10.1016/j.foodhyd.2011.01.009

20. Liu K, Liu Y, Lin D, Pei A, Cui Y (2018) Materials for lithium-ion battery safety. Sci Adv 4(6):eaas9820. https://doi.org/10.1126/sciadv.aas9820
21. Lisbona D, Snee T (2011) A review of hazards associated with primary lithium and lithium-ion batteries. Proc. Safety Environ. Protect 89(6), 434-442. https://doi.org/10.1016/j.psep.2011.06.022
22. Lee H, Yanilmaz M, Toprakci O, Fu K, Zhang X (2014) A review of recent developments in membrane separators for rechargeable lithium-ion batteries. Energy Environ Sci 7(12):3857–3886. https://doi.org/10.1039/C4EE01432D
23. Li W, Pang Y, Liu J, Liu G, Wang Y, Xia Y (2017) A PEO-based gel polymer electrolyte for lithium ion batteries. RSC Adv 7(38):23494–23501. https://doi.org/10.1039/C7RA02603J
24. Lawal OS, Lechner MD, Hartmann B, Kulicke WM (2007) Carboxymethyl cocoyam starch: Synthesis, characterisation and influence of reaction parameters. Starch-Stärke 59(5):224–233. https://doi.org/10.1002/star.200600594
25. Lin H, Van Wagner E, Swinnea JS, Freeman BD, Pas SJ, Hill AJ, Kalakkunnath S, Kalika DS (2006) Transport and structural characteristics of crosslinked poly (ethylene oxide) rubbers. J Membrane Sci 276(1–2):145–161. https://doi.org/10.1016/j.memsci.2005.09.040
26. Liu M, Wang Y, Li M, Li G, Li B, Zhang S, Ming H, Qiu J, Chen J, Zhao P (2020) A new composite gel polymer electrolyte based on matrix of PEGDA with high ionic conductivity for lithium-ion batteries. Electrochim Acta 354:136622. https://doi.org/10.1016/j.electacta.2020.136622
27. Liu M, Zhang S, Li G, Wang C, Li B, Li M, Wang Y, Ming H, Wen Y, Qiu J, Chen J, Zhao P (2021) A cross-linked gel polymer electrolyte employing cellulose acetate matrix and layered boron nitride filler prepared via in situ thermal polymerization. J Power Sourc 484:229235. https://doi.org/10.1016/j.jpowsour.2020.229235
28. Lin Z, Guo X, Wang Z, Wang B, He S, O'Dell LA, Huang J, Li H, Yu H, Chen L (2020) A wide-temperature superior ionic conductive polymer electrolyte for lithium metal battery. Nano Energy 73:104786. https://doi.org/10.1016/j.nanoen.2020.104786
29. Lizundia E, Kundu D (2021) Advances in Natural Biopolymer-Based Electrolytes and Separators for Battery Applications. Adv Funct Mater 31(3):2005646. https://doi.org/10.1002/adfm.202005646
30. Li S, Huang Y, Luo C, Ren W, Yang J, Li X, Wang M, Cao H (2020) Stabilize lithium metal anode through constructing a lithiophilic viscoelastic interface based on hydroxypropyl methyl cellulose. Chem Eng J 399:125687. https://doi.org/10.1016/j.cej.2020.125687
31. Liu FQ, Wang WP, Yin YX, Zhang SF, Shi JL, Wang L, Zhang X-D, Zheng Y, Jou J-J, Li L, Guo YG (2018) Upgrading traditional liquid electrolyte via in situ gelation for future lithium metal batteries. Sci Adv 4(10):eaat5383. http://doi.org/10.1126/sciadv.aat5383
32. Manthiram A (2017) An outlook on lithium ion battery technology. ACS Cent Sci 3(10):1063–1069. https://doi.org/10.1021/acscentsci.7b00288
33. Minaev KM, Martynova DO, Zakharov AS, Sagitov RR, Ber AA, Ulyanova OS (2016, September) Synthesis of Carboxymethyl Starch for increasing drilling mud quality in drilling oil and gas wells. In

IOP Conference Series: Earth and Environmental Science (Vol. 43, No. 1, p. 012071). IOP Publishing. https://doi.org/10.1088/1755-1315/43/1/012071

34. Murthy NS, Minor H (1990) General procedure for evaluating amorphous scattering and crystallinity from X-ray diffraction scans of semicrystalline polymers. Polymer 31(6):996–1002. https://doi.org/10.1016/0032-3861(90)90243-R
35. Naderi R (2016) Composite gel polymer electrolyte for lithium ion batteries. South Dakota State University
36. Nirmale TC, Karbhal I, Kalubarme RS, Shelke MV, Varma AJ, Kale BB (2017) Facile synthesis of unique cellulose triacetate based flexible and high performance gel polymer electrolyte for lithium ion batteries. ACS Appl Mater Interfaces 9(40):34773–34782. https://doi.org/10.1021/acsami.7b07020
37. Pereira AGB, Paulino AT, Nakamura CV, Britta EA, Rubira AF, Muniz EC (2011) Effect of starch type on miscibility in poly(ethylene oxide) (PEO)/starch blends and cytotoxicity assays. Mater Sci Eng C 31(2):443–451. https://doi.org/10.1016/j.msec.2010.11.004
38. Prinos J, Panayiotou C (1995) Glass transition temperature in hydrogen-bonded polymer mixtures. Polymer 36(6):1223–1227. https://doi.org/10.1016/0032-3861(95)93924-B
39. Rajeh A, Morsi MA, Elashmawi IS (2019) Enhancement of spectroscopic, thermal, electrical and morphological properties of polyethylene oxide/carboxymethyl cellulose blends: combined FT-IR/DFT. Vacuum 159:430–440. https://doi.org/10.1016/j.vacuum.2018.10.066
40. Song A, Huang Y, Zhong X, Cao H, Liu B, Lin Y, Wang M, Li X (2017) Gel polymer electrolyte with high performances based on pure natural polymer matrix of potato starch composite lignocellulose. Electrochim Acta 245:981–992. https://doi.org/10.1016/j.electacta.2017.05.176
41. Shen W, Li K, Lv Y, Xu T, Wei D, Liu Z (2020) Highly-Safe and Ultra-Stable All-Flexible Gel Polymer Lithium Ion Batteries Aiming for Scalable Applications. Adv Energy Mater 10(21):1904281. https://doi.org/10.1002/aenm.201904281
42. Thakur VK, Ding G, Ma J, Lee PS, Lu X (2012) Hybrid materials and polymer electrolytes for electrochromic device applications. Adv Mater 24(30):4071–4096. https://doi.org/10.1002/adma.201200213
43. Tang S, Lan Q, Xu L, Liang J, Lou P, Liu C, Mai L, Cao YC, Cheng S (2020) A novel cross-linked nanocomposite solid-state electrolyte with super flexibility and performance for lithium metal battery. Nano Energy 71:104600. https://doi.org/10.1016/j.nanoen.2020.104600
44. Vetter J, Novák P, Wagner MR, Veit C, Möller KC, Besenhard JO, Winter M, Wohlfahrt-Mehrens M, Vogler C, Hammouche A (2005) Ageing mechanisms in lithium-ion batteries. J Power Sourc 147(1–2):269–281. https://doi.org/10.1016/j.jpowsour.2005.01.006
45. Xue C, Jin D, Nan H, Wei H, Chen H, Zhang C, Xu S (2021) Ultrastable Lithium-Ion Batteries Prepared by Introducing γ-$LiAlO_2$ in a Gel Polymer Electrolyte at 50° C Working Temperature. ACS Appl Energy Mater 4(4):3633–3643. https://doi.org/10.1021/acsaem.1c00040
46. Yue L, Ma J, Zhang J, Zhao J, Dong S, Liu Z, Cui G, Chen L (2016) All solid-state polymer electrolytes for high-performance lithium ion batteries. Energy Storage Materials 5:139–164.

https://doi.org/10.1016/j.ensm.2016.07.003

47. Wang X, Zhai H, Qie B, Cheng Q, Li A, Borovilas J, Xu B, Shi C, Jin T, Liao X, Li Y, He X, Du S, Fu Y, Dontigny M, Zaghib K, Yang Y (2019) Rechargeable solid-state lithium metal batteries with vertically aligned ceramic nanoparticle/polymer composite electrolyte. Nano Energy 60:205–212. https://doi.org/10.1016/j.nanoen.2019.03.051
48. Zhou G, Li F, Cheng HM (2014) Progress in flexible lithium batteries and future prospects. Energy Environ Sci 7(4):1307–1338. https://doi.org/10.1039/C3EE43182G
49. Zhang Y, Lu W, Cong L, Liu J, Sun L, Mauger A, Julien CM, Xie H, Liu J (2019) Cross-linking network based on Poly(ethylene oxide): Solid polymer electrolyte for room temperature lithium battery. J Power Sourc 420:63–72. https://doi.org/10.1016/j.jpowsour.2019.02.090
50. Zhou J, Ji H, Liu J, Qian T, Yan C (2019) A new high ionic conductive gel polymer electrolyte enables highly stable quasi-solid-state lithium sulfur battery. Energy Storage Mater 22:256–264. https://doi.org/10.1016/j.ensm.2019.01.024
51. Zhao L, Fu J, Du Z, Jia X, Qu Y, Yu F, Du J, Chen Y (2020) High-strength and flexible cellulose/PEG based gel polymer electrolyte with high performance for lithium ion batteries. J Membrane Sci 593:117428. https://doi.org/10.1016/j.memsci.2019.117428
52. Zheng X, Liu K, Yang T, Wei J, Wang C, Chen M (2021) Sandwich composite PEO@(Er0.5Nb0.5)0.05Ti0.95O2@cellulose electrolyte with high cycling stability for all-solid-state lithium metal batteries. J Alloys Compounds 877:160307. https://doi.org/10.1016/j.jallcom.2021.160307
53. Zhu YS, Xiao SY, Li MX, Chang Z, Wang FX, Gao J, Wu YP (2015) Natural macromolecule based carboxymethyl cellulose as a gel polymer electrolyte with adjustable porosity for lithium ion batteries. J Power Sourc 288:368–375. https://doi.org/10.1016/j.jpowsour.2015.04.117
54. Zhou Q, Ma J, Dong S, Li X, Cui G (2019) Intermolecular chemistry in solid polymer electrolytes for high-energy-density lithium batteries. Adv Mater 31(50):1902029. https://doi.org/10.1002/adma.201902029
55. Zhao J, Chen D, Boateng B, Zeng G, Han Y, Zhen C, Goodenough JB, He W (2020) Atomic interlamellar ion path in polymeric separator enables long-life and dendrite-free anode in lithium ion batteries. J Power Sourc 451:227773. https://doi.org/10.1016/j.jpowsour.2020.227773

Figures

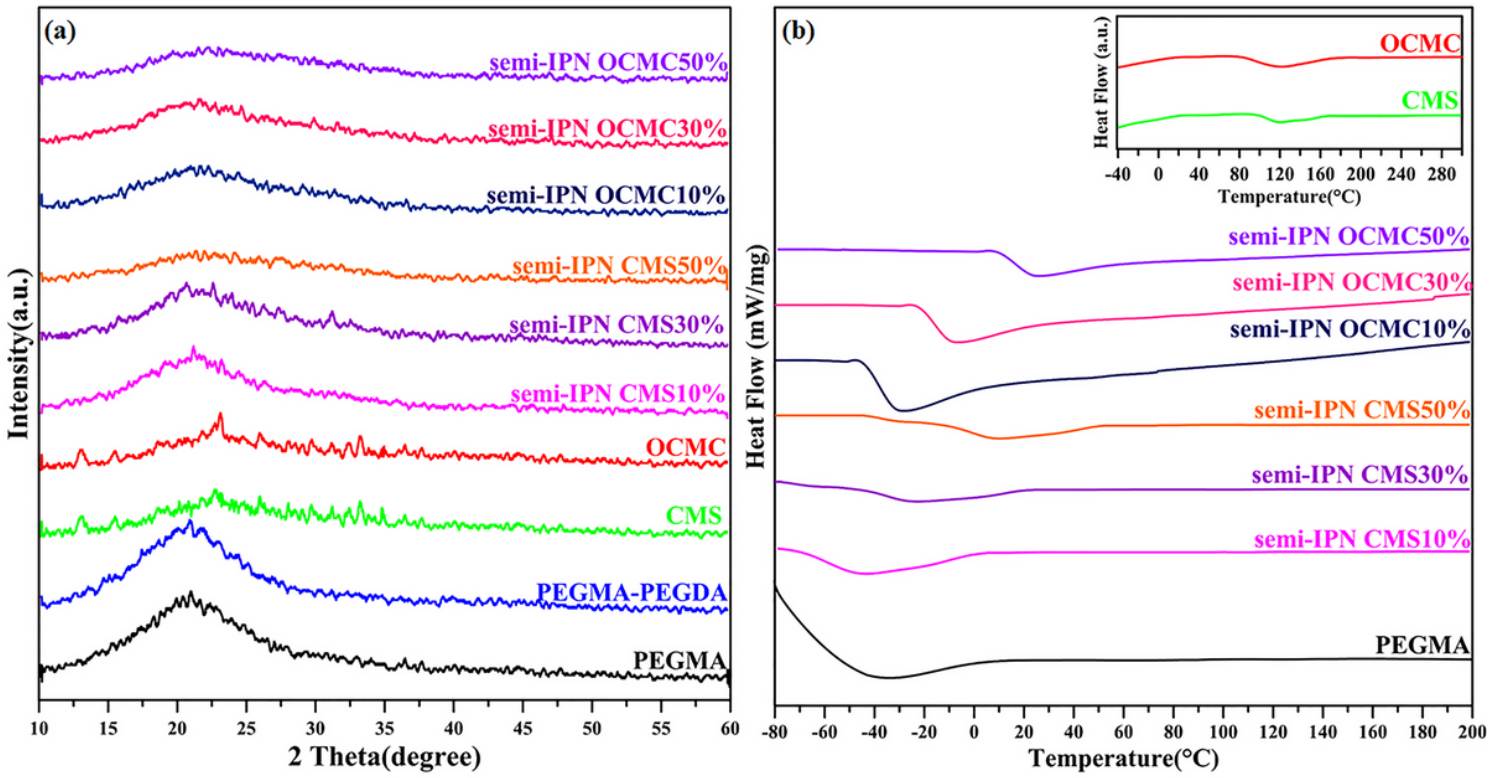

Figure 1

(a) XRD patterns and (b) DSC curves of PEGMA, PEGMA-PEGSA, semi-IPNs of CMS and OCMC in various ratios

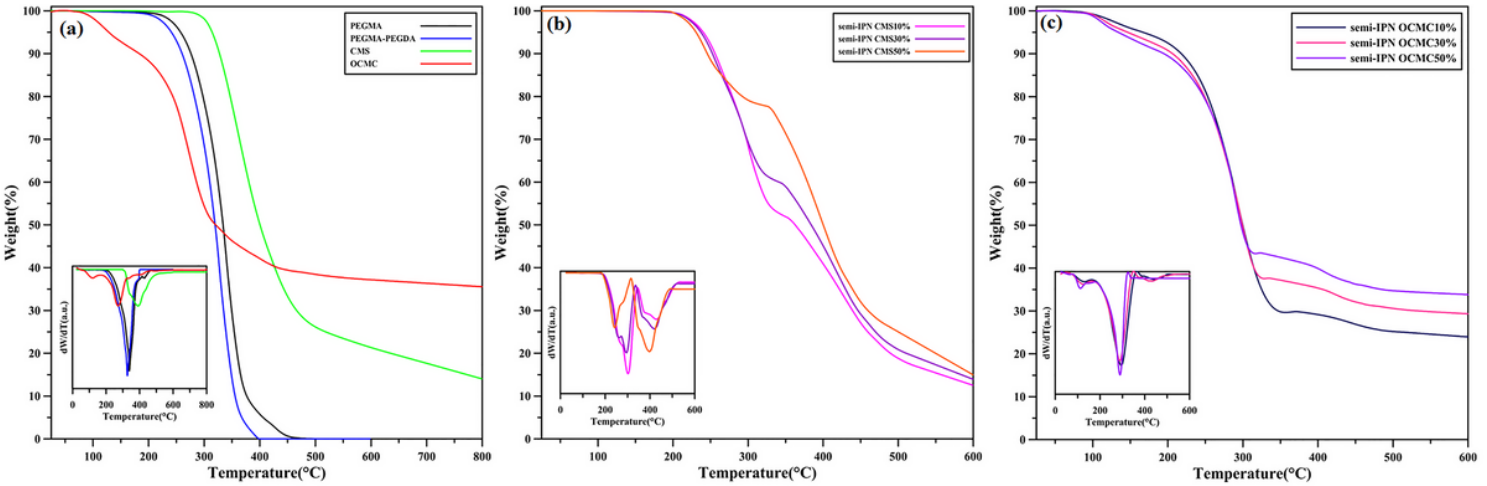

Figure 2

TGA curves of (a) PEGMA, PEGMA-PEGDA, CMS, and OCMC, (b) semi-IPNS of CMS, and (c), and semi-IPNs of OCMC

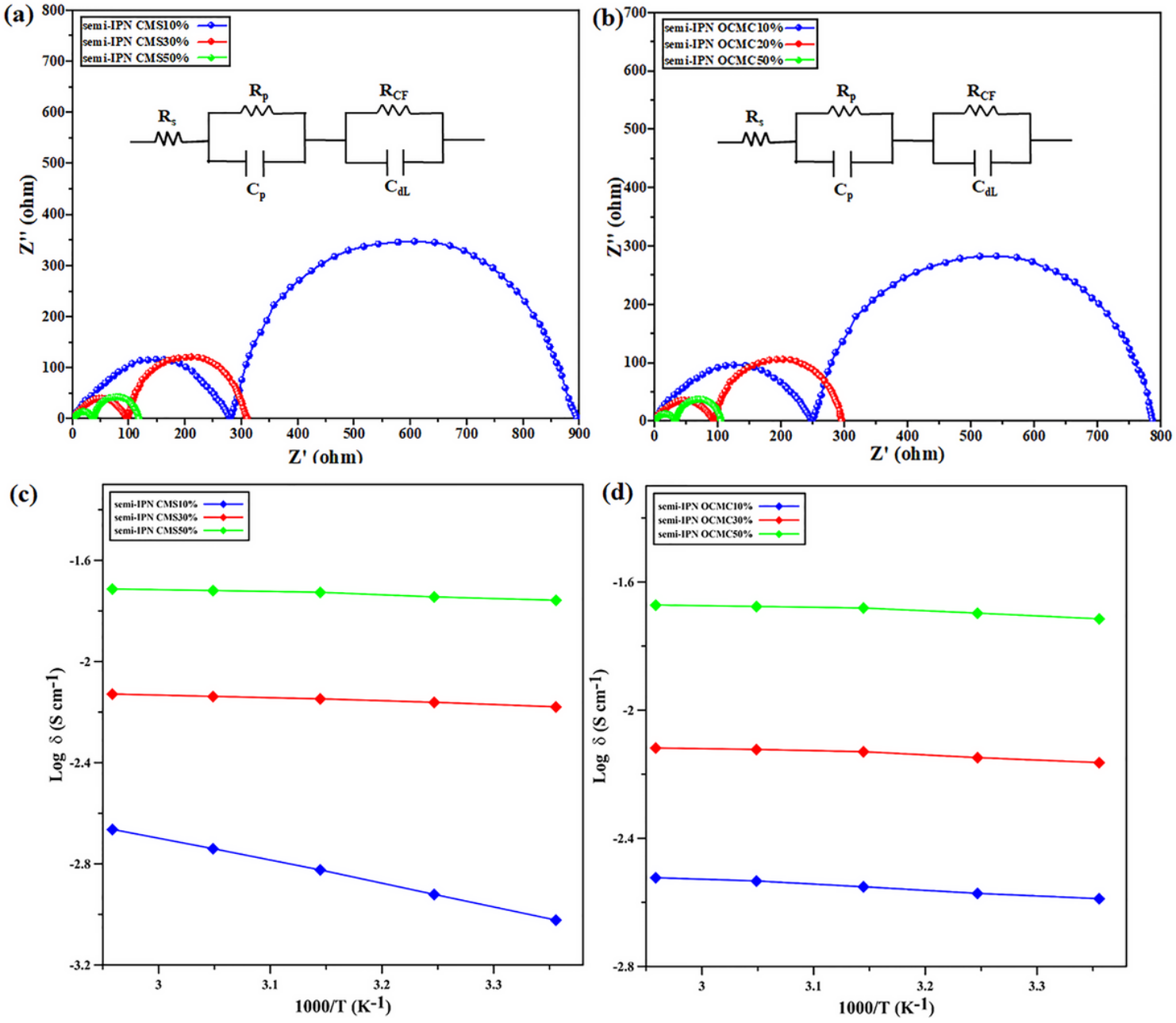

Figure 3

Impedance plots of SS/GPEs/SS at room temperature. (a) semi-IPNs CMS and (b) semi-IPNs OCMC with various ratios. Temperature ionic conductivity of the (c) semi-IPNS of CMS and (d) semi-IPNS of OCMC with various ratios obtained from Figure S4

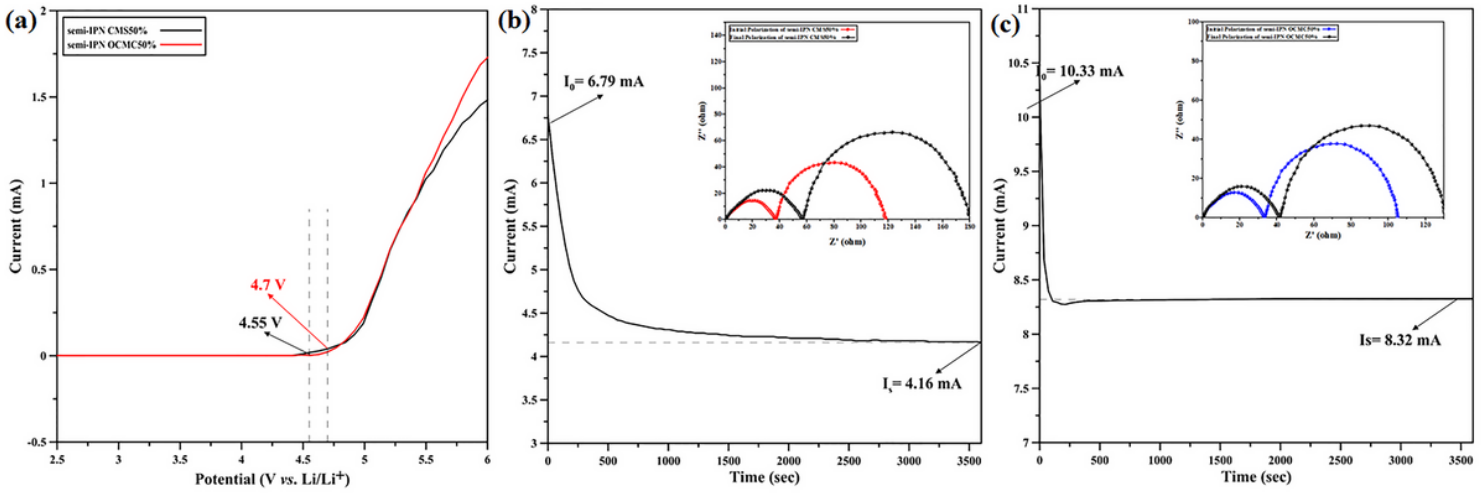

Figure 4

Cyclic voltammetry curves of (a) semi-IPNs for LiCoO2/GPE/Li cell. Chronoamperometry curves showing the time-dependence response of 10 mV DC polarization for a symmetric (b) Li/semi-IPN CMS50%/Li cell and (c) Li/semi-IPN OCMC50%/Li.

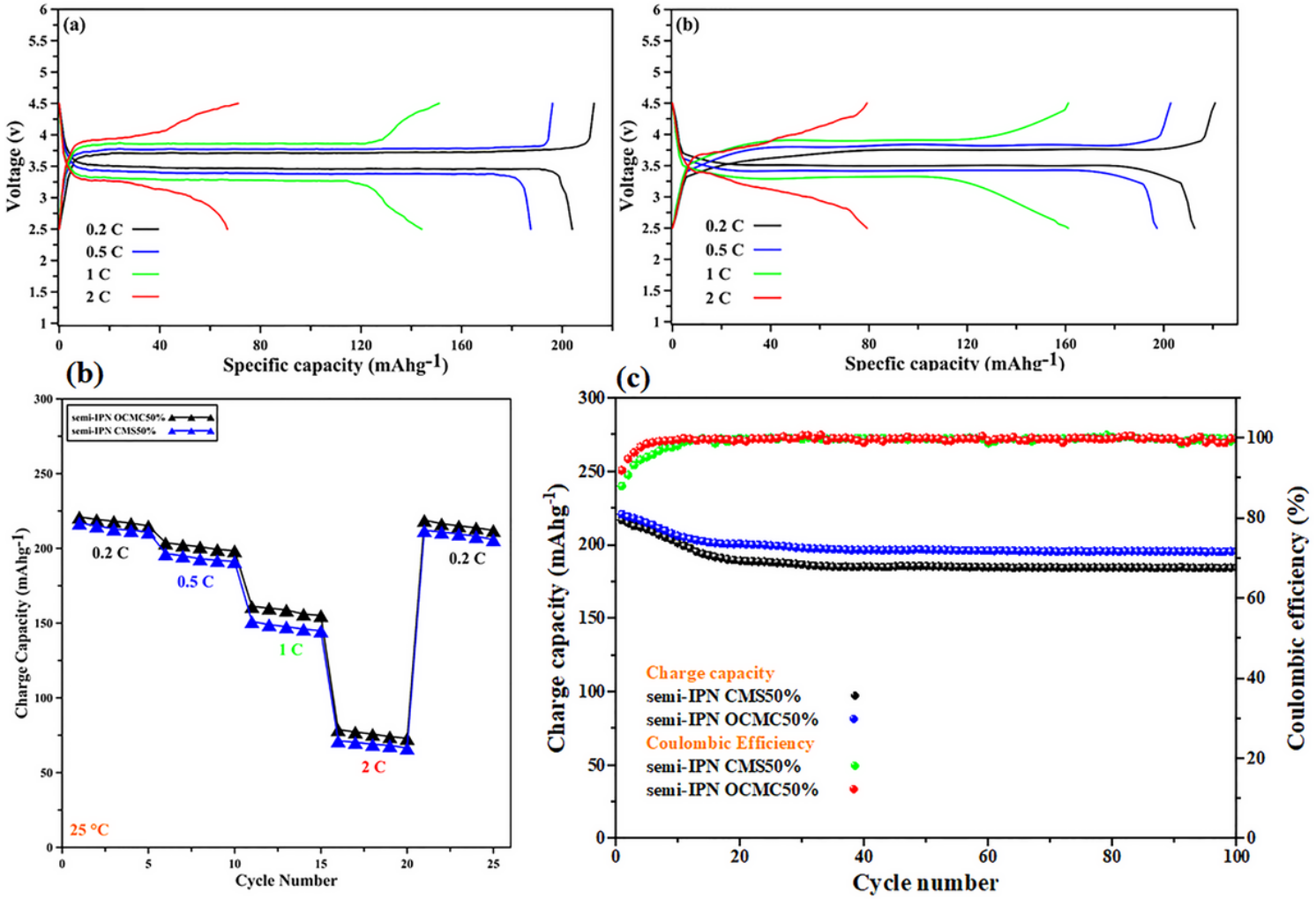

Figure 5

Galvanostatic charge–discharge profiles of (a) semi-IPN CMS50% and (b) semi-IPN OCMC50%. (c) Rate performance at various C rates, and (d) charge capacities and Coulombic efficiency at 0.1 C-rate at a voltage range between 2.5 and 4.5 V of the semi-IPN CMS50% and semi-IPN OCMC50% for LiCoO2/ GPE /Li

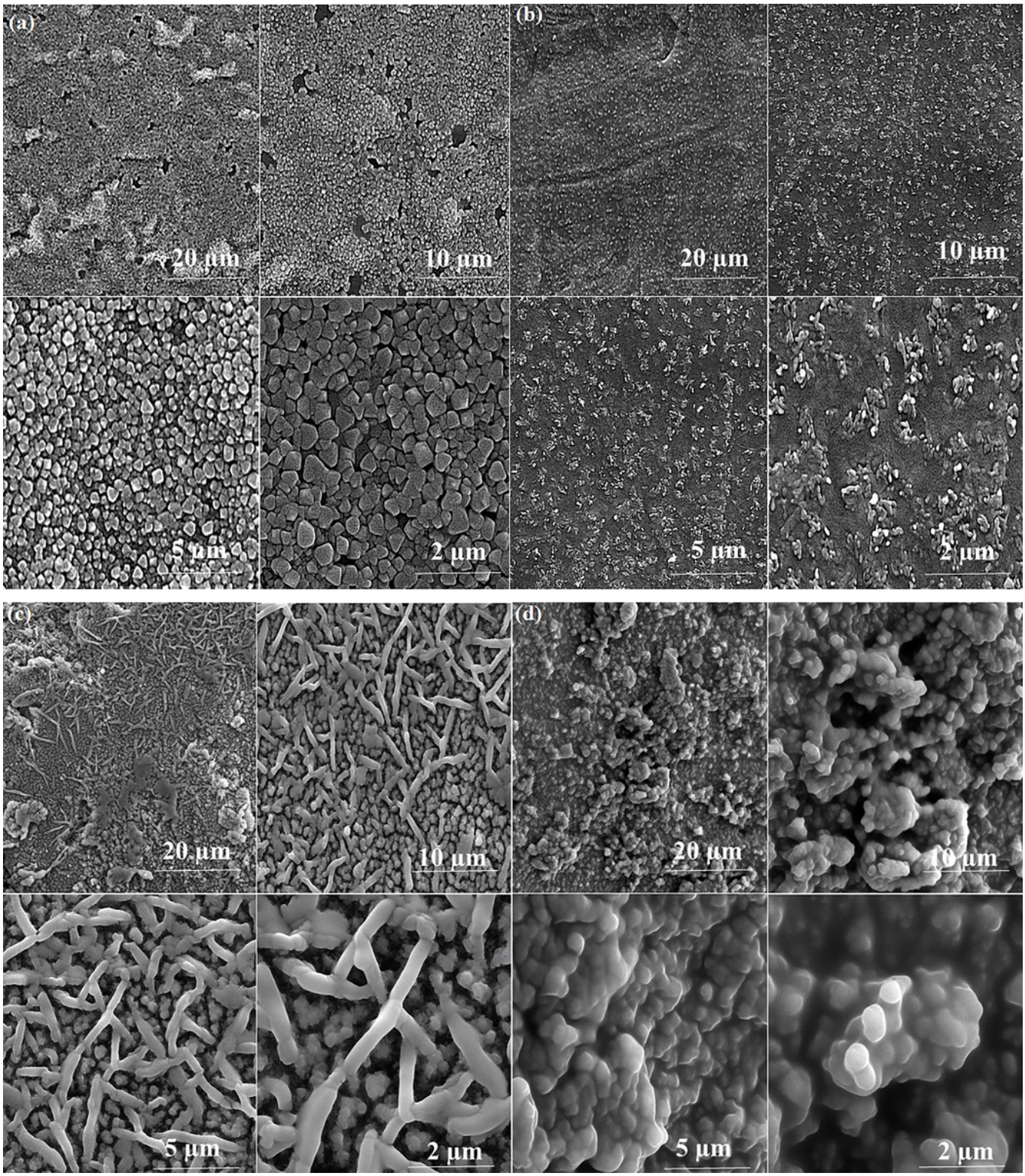

Figure 6

FE-SEM results of (a) semi-IPN CMS50% and (b) semi-IPN OCMC50% before charge and discharge, and (c) semi-IPN CMS50% and (d) semi-IPN OCMC50% after 100 cycles

Supplementary Files

This is a list of supplementary files associated with this preprint. Click to download.

- Scheme1.png
- SupportingInformation.docx